Transactions of the Korean Nuclear Society Spring Meeting
Jeju, Korea, May 18-19, 2023

Analysis of Reactivity Insertion Accident with the Multi-group Pin Homogenized SP_3 Code SPHINCS

Hyun Ho Cho[1)*] and Junsu Kang[2)]
Korea Atomic Energy Research Institute, 111, Daedeok-daero 989beon-gil, Yuseong-gu, Daejeon, 34057, Korea[1)]
Department of Nuclear Engineering and Radiological Science, University of Michigan, Ann Arbor, MI, USA[2)]
[*]Corresponding author: h2joh33@kaeri.re.kr

1. Introduction

The conventional assembly-wise two-step method has long been used as a practical tool for nuclear design and analyses due to its low computing cost. Nevertheless, the pin-wise two-step method has attracted attention as a way to reduce the errors arising from assembly-wise homogenization. Therefore, with the help of growth of computing power, the core analyses methods based on pin-wise two-step method is being widely developed recently [1,2]. In the pin-by-pin core analyses, the region of spatial homogenization is reduced from fuel assembly to fuel pin, which means that the pin power distribution can be obtained directly without the need for pin power reconstruction.

In this regard, the second class of pin-wise two-step method was developed by combining the nTRACER direct whole core calculation code (DWCC) [3] and the SPHINCS multi-group pin homogenized simplified P_3 (SP_3) code [2]. Although nTRACER was originally developed for DWCC employing the planar method of characteristics (MOC) based on coarse mesh finite difference (CMFD) formulation, it can be used as a lattice transport code to generate assembly or pin homogenized group constants (AHGCs or PHGCs). SPHINCS was developed employing the pin-level 2D/1D finite difference method (FDM) coupled with the assembly-level CMFD. In SPHINCS, the pin-wise super homogenization (SPH) factors are used to alleviate not only the homogenization error, but also the spatial truncation error associated with the use of pin sized FDM meshes.

The C5G7-TD benchmark [4], which consists of six sets of transient benchmark problems without thermal/hydraulic (T/H) feedbacks, was proposed to examine the accuracy of the spatial kinetics solutions. Through the application of SPHINCS to the C5G7-TD benchmark problems, it was confirmed that the pin-wise two-step calculations can successfully generate accurate transient solutions even for the heavily rodded cases [5]. To continue the verification and validation of the transient capability of SPHINCS, realistic dynamic problems which involve T/H feedbacks were required to be analyzed. In this regard, the 5x5 mini-core problem, which postulates the reactivity insertion accident (RIA) transient states including T/H feedbacks [6] was analyzed using SPHINCS. The accuracy of SPHINCS pin homogenized SP_3 solutions was assessed by the comparison with nTRACER direct whole core transport solutions.

2. Problem specifications

2.1. Core modeling and transient scenario

The model consists of an asymmetric 5x5 fuel assembly array as shown in Fig. 1, in which three types of 17x17 pin-cell assemblies are loaded with reflective boundary conditions. Three types of fuel assembly have different enrichment and two of them have other cases that the control rod is inserted. The detailed core configurations are given in the reference [6]. Reflective boundary conditions are used in both radial and axial directions and the initial core state is set as critical by adjusting the boron concentration in moderator.

In the reference [6], super-prompt critical RIA was initiated by the instantaneous ejection of a control rod located at the periphery of the core as shown in Fig. 1. The rod worth of the ejected control rod was 1.21$. However, since not all the material compositions were provided in the reference [6], core modeling was done with some assumptions and the control rod worth was set to 1.28$. Also, the instantaneous ejection of control rod was replaced by linear rod ejection up to 0.1s for the calculation stability.

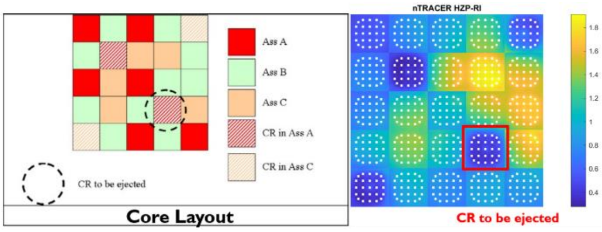

Fig. 1. Layout of 5x5 mini-core problem (left) [6] and pin power distribution for rodded condition obtained by nTRACER (right)

2.2. Previous research using DeCART/PARCS

In the previous research [6], the two-step core analysis was performed by using the PARCS [7] code which is one of the typical nodal core simulators, and the DeCART [8] code which provides direct whole core solutions. The DeCART/PARCS analysis was performed based on the AHGCs with discontinuity factors (DFs) generated from full-core heterogeneous solutions. A set of branch calculations were performed at the full-core level as well. Contrary to that, for the nTRACER/SPHINCS analysis in this study, only five sets of single fuel assembly (SA) were used to generate

Table I: Comparison of initial core states and control rod worth for 5x5 mini-core problem between SPHINCS and nTRACER

Description	HZP-RI				HZP-RO				Rod worth (pcm)	
	Reactivity		Pin pow. diff. (%)		Reactivity		Pin pow. diff. (%)			
	k-eff.	Δρ	Max.	RMS	k-eff.	Δρ	Max.	RMS	Value	Difference
nTRACER	0.99999	-	-	-	1.01177	-	-	-	1164.3	-
SPHINCS(2G)	1.00161	162	-3.64	1.23	1.01282	102	-3.38	1.20	1105.0	-59.3
SPHINCS(4G)	1.00041	42	-2.03	0.52	1.01206	28	-2.31	0.50	1150.6	-13.7
SPHINCS(8G)	1.00018	19	-1.63	0.44	1.01191	14	-1.53	0.45	1159.0	-5.3

PHGCs and then SPH factors were generated from the identical five sets of SA calculation.

2.3. Generation of PHGCs and kinetic parameters

PHGCs were obtained by the heterogeneous lattice transport solver, nTRACER, which uses a fine energy group structure (EGS) of 47 group (47G). In the lattice transport calculations, explicitly modeled assemblies were used in infinite medium condition. Each pin-cell in the assembly was divided into tens of flat source regions (FSRs) and the resulting FSR-wise fluxes were used to generate PHGCs. PHGCs were condensed into a few EGS to be used in lower order solver, SPHINCS. Three types of EGS were compared and the lower energy bounds of EGS are given in Table II.

Table II: Three types of energy group structure

2G	4G	8G	Lower energy bound (eV)
1	1	1	2.2313E+06
		2	8.2085E+05
		3	9.1188E+03
	2	4	1.3007E+02
		5	3.9279E+00
	3	6	6.2506E-01
2	4	7	1.4572E-01
		8	0.0000E+00

With the given PHGCs and pin-wise fluxes, the group-wise SPH factors for each pin were obtained in an iterative procedure while preserving the group-wise total reaction rates at each pin. The SPH factors were then incorporated into corresponding PHGCs and used for the core analysis.

For the delayed neutron source terms, the six groups of delayed neutron precursor were used while the precursor decay constants and delayed neutron group spectra were the same as nTRACER. The delayed neutron fractions were homogenized, and group condensed using a fission source as a weighting factor. The neutron velocities were obtained by homogenization and group condensation of the inverse of neutron velocities using the neutron flux as a weighting factor.

In the super-prompt critical RIA, the Doppler effect becomes the major negative feedback mechanism as the fuel temperature increases. In order to properly account for the Doppler effect, the effective fuel temperature, i.e. the effective Doppler temperature, was used. The effect of weighting factor in the effective Doppler temperature was investigated in Section 4.3.

3. Analysis of steady state results

The initial core state was analyzed in terms of multiplication factor, pin power, and control rod worth at the hot zero power conditions with control rod inserted (HZP RI) and withdrawn (HZP RO). SPHINCS steady state results were successfully generated using PHGCs and SPH factors obtained from SA calculations. While 2G AHGCs have been widely used in typical nodal calculations, it turned out that 8G EGS is better suited for PHGCs. The reduction of pin power discrepancy according to the use of 8G EGS rather than 2G was clearly shown as shown in Fig. 2. The 8G EGS significantly improved the rod worth accuracy as well. The discrepancy of about -60pcm of 2G EGS was reduced to about -5pcm when using 8G EGS as represented in Table I. Therefore, during the rod ejection transient, it can be said that the difference in the power rise and energy deposition between SPHINCS and nTRACER depends on the kinetic parameters.

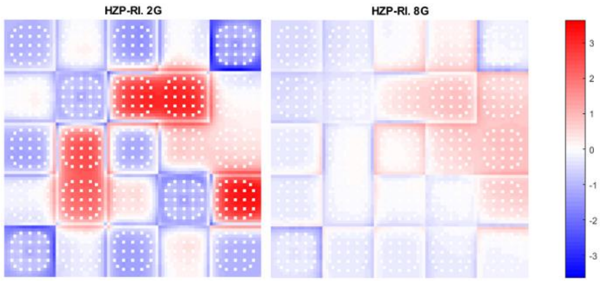

Fig. 2. Differences in pin power distribution for 2G (left) and 8G (right) EGS compared to the nTRACER results

4. Assessment of transient solutions

4.1. RIA without T/H feedbacks

Transient calculations without T/H feedbacks were performed to assess the EGSs and verify the kinetic parameters. Without T/H feedbacks, the core power rises exponentially. The neutron balance equation at the critical state with the six groups of delayed neutron precursor can be written with the distinction between prompt and delayed neutrons as follows:

$$\frac{1}{v}\frac{d\phi}{dt} = \left(\nu\Sigma_f - \Sigma_a - \nu_d\Sigma_f\right)\phi + \sum_{k=1}^{6}\lambda_k C_k,$$
$$\Lambda\frac{d\phi}{dt} = \left(\rho - \beta\right)\phi + \sum_{k=1}^{6}\lambda_k \frac{C_k}{\nu\Sigma_f}, \quad (1)$$

where neutron generation time $\Lambda = \frac{1}{v \cdot \nu\Sigma_f}$, reactivity $\rho = 1 - \frac{\Sigma_a}{\nu\Sigma_f}$ and delayed neutron fraction $\beta = \frac{\nu_d}{\nu}$ are applied.

Here, the inverse period defined as Eq. (2), which corresponds to the slope of the power rise shown in the semi-log scale versus time is compared in Fig. 3. As same as initial core state analysis, as the number of EGS increases, the inverse period of SPHINCS showed great agreement compared to that of nTRACER. The inverse period with the 2G EGS showed lowest inverse period which was induced by most under-estimation of inserted reactivity after the control rod ejection.

$$\alpha = \frac{\rho - \beta}{\Lambda}. \qquad (2)$$

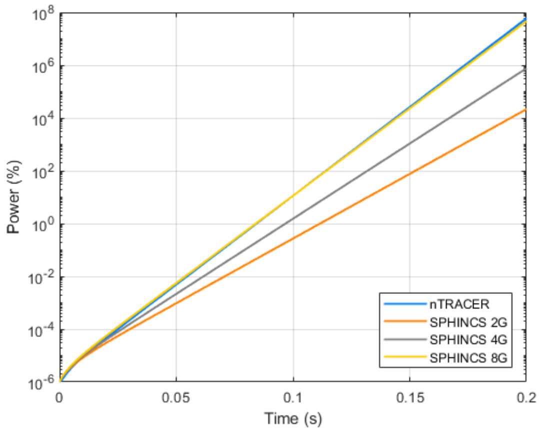

Fig. 3. Core power change for RIA without T/H feedbacks

Table III: Comparison of inverse periods for RIA without T/H feedbacks

Description	α (s^{-1})	Relative Diff. (%)
nTRACER	155.52	-
SPHINCS (2G)	113.97	-26.72
SPHINCS (4G)	132.08	-15.07
SPHINCS (8G)	153.09	-1.56

4.2. RIA with T/H feedbacks

With T/H feedbacks, the elevated core power after reactivity insertion is expected to be decreased to an asymptotic power level since the negative fuel temperature coefficient feedback will compensate the inserted positive reactivity. The fuel temperature change of SPHINCS with 8G EGS showed better agreement than that with 2G or 4G EGS compared to that of nTRACER as shown in Fig. 4. As shown in Fig. 5, the dynamic reactivity which was obtained through weighting the reactivity with adjoint fluxes was measured and the dynamic reactivity behavior showed great agreement with 8G EGS as well. Then, the core power behavior was compared as shown in Table IV and Fig. 6. For both aspects of the maximum core power and the time at which peak power is reached, the results of SPHINCS with 8G EGS showed great agreement. Therefore, 8G EGS is required in pin-by-pin core analysis not only for the steady states but also for the transient states.

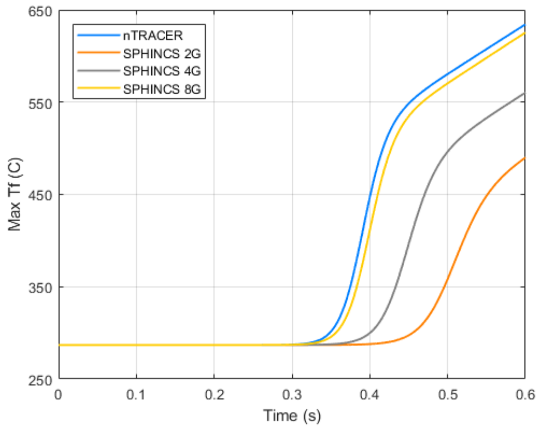

Fig. 4. Fuel temperature change for RIA with T/H feedbacks

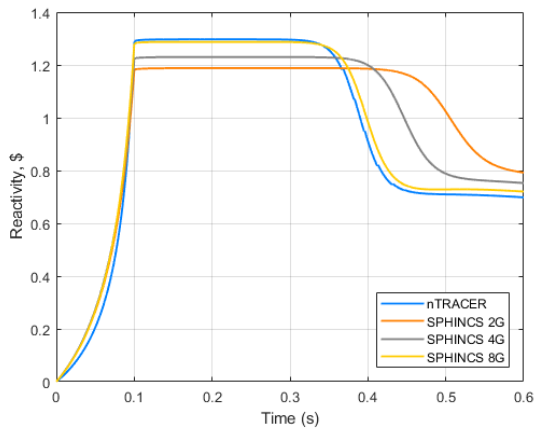

Fig. 5. Dynamic reactivity change for RIA with T/H feedbacks

Table IV: Comparison of peak time and peak core power for RIA with T/H feedbacks

Description	Peak time (s)		Peak power (%)	
nTRACER	0.391	Abs. Diff.	1672.7	Rel. Diff.
SPHINCS(2G)	0.510	+0.119	903.9	-46.0
SPHINCS(4G)	0.449	+0.058	1268.9	-24.1
SPHINCS(8G)	0.400	+0.009	1692.1	+1.2

4.3. Impact of the effective Doppler temperature

Since the fuel temperature coefficient is responsible for the most important feedback that will compensate the inserted positive reactivity due to the control rod ejection, it is important to estimate the fuel temperature properly. In the direct whole core calculation of nTRACER, intra-pellet fuel temperature profile was explicitly considered using tens of concentric circles. However, in SPHINCS, the temperature profile was assumed to be spatially flat.

Therefore, to account for the fuel temperature spatial distribution, the effective Doppler temperature was used in SPHINCS. The effective Doppler temperature of a specific pin is defined as:

$$T_F^{eff} = \omega T_F^{VA} + (1-\omega) T_F^{PS} \quad (3)$$

where T_F^{VA} is a volume averaged fuel temperature, T_F^{PS} is a fuel pellet surface temperature, and ω is a weighting factor so-called the Studsvik factor. The Studsvik factor of 1.0 corresponds to the conventional volume averaged fuel temperature. The Studsvik factor was determined by the comparison of reactivity between nTRACER and SPHINCS steady state calculations. The comparison of reactivity using various Studsvik factors was shown in Fig. 7. The factor of 0.97 showed the best agreement between nTRACER and SPHINCS in the core problem. The impact of effective Doppler temperature was analyzed for the accuracy of peak time, peak power and asymptotic power level as shown in Table V. The factor of 0.97 showed the best agreement with nTRACER as it was in steady state calculation.

Table V: Impact of effective fuel temperature to the peak time, peak core power and asymptotic core power

	ω	Peak time (s)		Peak power (%)		Asymptotic power (%)	
nT.	-	0.391	Abs. Diff.	1672.7	Abs. Diff.	229.7	Rel. Diff.
SP.	1.00	0.400	+0.009	1692.1	+1.2	224.9	-2.1
	0.97	0.400	+0.009	1699.7	+1.6	229.3	-0.2
	0.96	0.400	+0.009	1702.3	+1.8	230.8	+0.5
	0.95	0.400	+0.009	1704.8	+1.9	232.4	+1.2
	0.94	0.400	+0.009	1707.4	+2.1	234.0	+1.9

5. Conclusions

Through the analysis of super-prompt RIA with the multi-group pin homogenized SP_3 code SPHINCS, it was confirmed that the core power excursion and subsequent negative reactivity feedback due to the control rod ejection can be analyzed with sufficient accuracy. The PHGCs, SPH factors, and kinetic parameters with 8G EGS generated from the sets of SA calculations can properly estimate the changes in fuel temperature, core power, and dynamic reactivity. Also, with careful determination of the effective Doppler temperature, the asymptotic power level showed great agreement with nTRACER.

ACKNOWLEDGEMENT

This work was supported by the National Research Foundation of Korea (NRF) funded by the Korea Government (Ministry of Science and ICT) (NRF-2020M2D7A1079181).

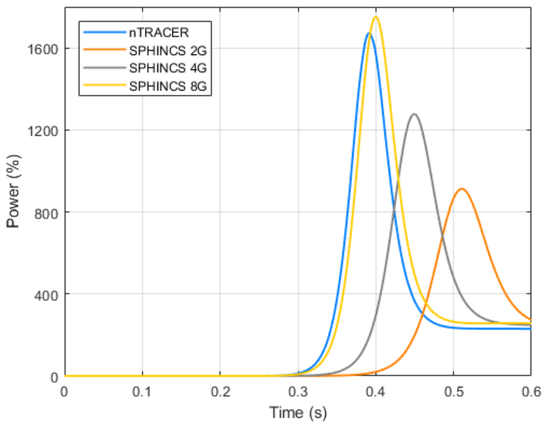

Fig. 6. Core power change for RIA with T/H feedbacks

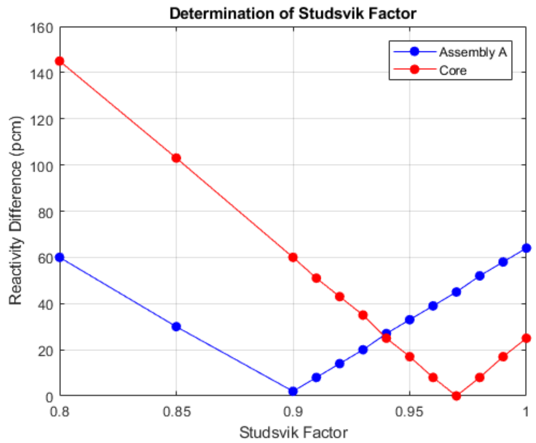

Fig. 7. Determination of Studsvik factor considering SA and core geometry

REFERENCES

[1] J. I. Yoon, et al., High performance 3D pin-by-pin neutron diffusion calculation based on 2D/1D decoupling method for accurate pin power estimation, Nuclear Engineering and Technology, Vol. 53, No. 11, pp. 3543-3562, 2021

[2] H. H. Cho, et al., Preliminary Development of Simplified P3 based Pin-by-pin Core Simulator SPHINCS, Transactions of the Korean Nuclear Society Spring Meeting, Jeju, Korea, May 23-24, 2019

[3] Y. S. Jung, et al., Practical Numerical Reactor Employing Direct Whole Core Neutron Transport and Subchannel thermal/hydraulic solvers, Annals of Nuclear Energy, Vol. 62, pp.357-374, 2013.

[4] V. F. Boyarinov, et al., Deterministic Time-Dependent Neutron Transport Benchmark without Spatial Homogenization (C5G7-TD), NEA/NSC/DOC, 2016.

[5] H. H. Cho, et al., Analysis of C5G7-TD benchmark with a multi-group pin homogenized SP3 code SPHINCS, Nuclear Engineering and Technology, Vol. 53, No. 5, pp. 1403-1415, 2021

[6] M. Hursin, et al., Assessment of assembly homogenized two-step core dynamic calculations using direct whole core transport solutions, Annals of Nuclear Energy, Vol. 87, pp. 356-365, 2016

[7] H. G. Joo, et al., PARCS: A Multi-Dimensional Two-Group Reactor Kinetics Code Based on the Nonlinear Analytic Nodal Method, PU/NE-98-26, 1998

[8] H. G. Joo, et al., Methods and Performance of a Three-Dimensional Whole-Core Transport Code DeCART, Proceedings of the PHYSOR 2004, Chicago, Illinois, USA, April 25-29, 2004